

Ufuk Senturk
Rogerio S. Lima

Center for Thermal Spray Research,
Department of Materials Science
and Engineering,
State University of New York at Stony Brook,
Stony Brook, NY 11794-2275

Carlos R. C. Lima

UNIMEP Methodist University of Piracicaba,
Technology Center,
Rod. Santa Barbara-Iracemapolis, Km 1,
Santa Barbara d'Oeste, S. Paulo, 13450-000,
Brazil

Christopher C. Berndt

Center for Thermal Spray Research,
Department of Materials Science
and Engineering,
State University of New York at Stony Brook,
Stony Brook, NY 11794-2275

Deformation of Plasma Sprayed Thermal Barrier Coatings

The deformation behavior of thermally sprayed partially stabilized zirconia (PSZ) coatings are investigated using Hertzian indentation and four-point bend testing, with in situ acoustic emission monitoring. The experimental deformation curves, together with the corresponding acoustic emission responses and the fracture properties of the material are used in defining the deformation characteristics of the coating (ceramic overlay with metallic bond coat where applicable) and substrate composite system. Experiments are aimed in examining the influence of the bond coat and the coating properties on the form of deformation. Substrate temperature and pauses during spraying are demonstrated to strongly effect the coating properties and the resulting fracture/failure characteristics of the composite system. [S0742-4795(00)02503-5]

Keywords: Plasma Spray, PSZ, Coating, Acoustic Emission, Mechanical Property

Introduction

Thermal Barrier Coatings (TBCs) have been widely used in gas turbine and diesel engines [1]. The most common material used as an insulator in such systems has been partially stabilized zirconia (PSZ), mainly for its low thermal conductivity and diffusivity combined with its high temperature stability. The general practice in preparing thermal spray TBCs is to spray the ceramic overlay onto a metallic bond coat layer, generally by plasma spraying for large components. Plasma sprayed TBCs experience high thermal stresses under service conditions due to cyclic thermal changes. Thermal stresses are generated mainly due to the thermal expansion coefficient mismatch between the ceramic coating and the metallic substrate. From the viewpoint of structural integrity and mechanical behavior, the presence of a metallic bond coat layer between the ceramic and substrate can reduce the effect of such stresses [2]. In addition, plasma sprayed TBCs are subjected to residual stresses that arise from the rapid cooling of molten or partially molten droplets impacting on the cool substrate, from thermal gradients, and from solid state transformations of the coating material. Hence, controlling the substrate temperature during deposition has a significant influence on the nature and magnitude of residual stresses [3–5].

Several approaches have been used to improve the mechanical properties, and thermal cycle and oxidation resistance behavior of TBCs [6–8]. These include (i) optimizing Young's modulus, (ii) reducing the thermal expansion coefficient mismatch between the coating and substrate, and (iii) increasing the oxidation resistance, especially near the substrate interface, at high temperatures. To better understand the coating formation and failure mechanisms, the influence of spray conditions and TBC system design have been characterized by a number of distinct methods. Acoustic Emission (AE) technology has been widely used as a non-

destructive method in characterizing the cracking and failure behavior of the coatings. The technique also has potential for the quality control and in-service monitoring of coatings during application or production. The method has mostly been used to understand the failure mechanisms during thermal cycling [9,10]. Less effort has been spent in characterizing the deformation and failure behavior at room temperature conditions, under mechanical stresses. Among the few studies, experiments have monitored the *in situ* cracking of samples during three-point [11,12] and four-point bend tests [13–15], tensile adhesion tests [16–20], and indentation [21] tests.

In this paper, the mechanical properties and cracking features of yttria stabilized zirconia (YSZ) ceramic coatings, either with or without a bond coat (NiCrAl) layer, plasma sprayed on plain carbon steel substrates are investigated. Four point bending and Hertzian indentation tests have been used to evaluate the mechanical response, while acoustic emission (AE) has been used to *in situ* monitor the cracking behavior during these tests. The bend tests are used to provide more quantitative results with respect to the mechanical properties of the coating-substrate system. The indentation tests are used for the simple determination of indentation loads that lead to failure and to gather general information about the deformation and adhesion behavior, which complement the information obtained from the bend tests. The mechanical tests are performed on coatings that were produced under processing conditions identified as either "cooling" or "no cooling" during the spray procedure are examined. Moreover, two types of coating structures are distinguished with coatings produced by a continuous spraying procedure and by a paused scheme.

Experimental Procedures

Materials and Spray Conditions. The coatings were air plasma sprayed (APS) using the conditions given in Table 1 with the plasma spray gun (Metco 3MB, Westbury, NY) mounted on a six-axis articulated robot (GMF Fanuc, Model S400). The feedstock material was yttria stabilized zirconia (YSZ), of average particle size of 56.2 μm for the top coat and NiCrAl for the bond coat, both externally injected into the plasma at a rate of 40 g/min using nitrogen as the carrier gas. Spraying was performed on mild

Contributed by the International Gas Turbine Institute (IGTI) of THE AMERICAN SOCIETY OF MECHANICAL ENGINEERS for publication in the ASME JOURNAL OF ENGINEERING FOR GAS TURBINES AND POWER. Paper presented at the International Gas Turbine and Aeroengine Congress and Exhibition, Indianapolis, IN, June 7–10, 1999; ASME Paper 99-GT-348. Manuscript received by IGTI March 9, 1999; final revision received by the ASME Headquarters May 15, 2000. Associate Technical Editor: D. Wisler.

Table 1 Plasma spray conditions

	YSZ	NiCrAl
Gun Type	Metco 3MB	Metco 3MB
Current	600A	500A
Voltage	70V	70V
Primary Gas	Ar(40 l/min)	Ar(40 l/min)
Secondary Gas	H ₂ (8 l/min)	H ₂ (1 l/min)
Powder Carrier Gas	N ₂ (3.5 l/min)	N ₂ (3.65 l/min)
Spray Distance	100mm	100mm

steel substrates of 60×7×2.54 mm size, providing it with the bond coat layer, where applicable, and the YSZ topcoat. Prior to spraying, the surfaces to be sprayed were grit blasted and washed in ethyl alcohol. For spraying, the samples were placed on a carousel with six substrates sprayed at a time. The rotation speed of the carousel was set at 160 rpm, while the robot was programmed to provide a vertical traverse distance of 90 mm at 12 mm/s. For samples where a bond coat layer was produced, the robot was set to repeat 10 uninterrupted passes, giving a thickness of 150–200 μm. For the YSZ topcoat, the spray gun was set to repeat a total of 100 passes, giving a thickness in the 900–1100 μm range. During the application of the ceramic coating, samples were coated in a continuous as well as in a paused schedule. For the continuous coatings, the spraying was performed without any interruptions until the desired thickness was reached. For the paused coatings, the spraying was stopped for 2 times (both after 40 passes) where the samples were allowed to cool to –100 °C; afterward the coating process was resumed until the desired thickness was achieved. It should be noted that for both the continuous and paused coatings, the thicknesses of the bond coat and ceramic layer was the same.

Coatings that were prepared continuously or with pauses were sprayed either with or without external cooling applied using pressurized air jets to maintain a constant substrate temperature. The temperature of the substrate was determined using temperature indicating liquids in different measuring ranges (Omegalag, Omega Engineering, Stamford, CT) and was confirmed using a hand held infrared temperature detector. The temperatures measured were in the 400–500 °C range for the "cooled" samples and was above 500 °C for the "non-cooled". It is also important to note the difference in the heating rates when making a distinction between the two cases. Samples having "bond coat" and "no bond" coat were made for the different cases described above.

Mechanical Testing and Acoustic Emission

Four Point Bending Tests. The samples were subjected to four-point bending (20 mm inner span and 40 mm outer span) using a servo-hydraulic testing machine (Model 8502, Instron, Canton, MA), with the crosshead speed set to 10 μm/sec and the load and displacement recorded for each measurement. A maximum load of 1 kN was applied to all the samples. A compliance calibration for the experimental arrangement was made using the Instron LVDT and an external LVDT (Model CD375-500, Macro Sensors, Pennsauken, NJ) that was placed close to the pin supports. This enabled a better measurement of displacement by calibrating the crosshead movement. During the tests, a piezoelectric AE transducer (pico-transducer, Physical Acoustics, Princeton, NJ) with a resonance frequency of 250 kHz was placed on the coating. The sensor was attached to a preamplifier (model 140B, Hartford Steam Boiler Inspection Technologies, Sacramento, CA) and a preamplifier filter (model FL12Y, Hartford Steam Boiler Inspection Technologies, Sacramento, CA), with an amplification of 40 dB and the frequency range analyzed at 10 kHz–1 MHz. The signal output was processed using an AET 5500 system (Hartford Steam Boiler Inspection Technologies, Hartford, CT), which was connected to a redundant PC to record the acoustic emission (AE)

responses. Procedures with regards to the experimental setup and AE signal processing are available elsewhere [14]. A total of two samples were tested for each condition. Prior to testing, the sample surfaces were polished to a 1 μm diamond finish and the specimens were stored in a desiccator. Blank steel substrates were also tested to examine the influence of the coating on the acoustic emission activities so that the acoustic emission contribution from the substrate could be taken into account.

Hertzian Indentation Tests. Hertzian (spherical) indentation tests were performed using an experimental set-up built on a servo-hydraulic testing machine (Model 8502, Instron, Canton, MA). This enabled load and displacement data to be collected during the indentation cycle, with the load detected using a load cell and the displacement using an external LVDT (Model CD375-500, Macro Sensors, Pennsauken, NJ). The LVDT in this case was placed close to the indenter tip so that the displacements from the indenter penetration can be more accurately measured. The indentations were performed using a 3.175 mm (1/8") diameter WC ball. The crosshead speed during the indentation cycle was set to 10 μm/s and a maximum load of 3 kN was applied to all the samples (Note: some coatings failed before this maximum load). The same AE transducer and data analysis system was used for both the four-point bending and indentation tests.

Results and Discussions

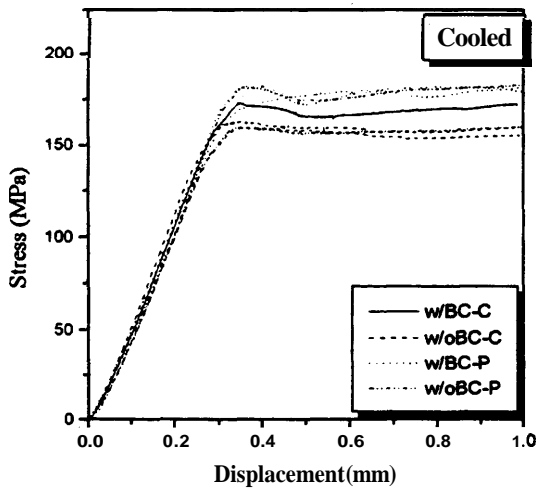
Four-Point Bending and Acoustic Emission. The stress-displacement curves for the "cooled" and the "non-cooled" coated samples are shown in Fig. 1(a) and Fig. 1(b), respectively. Stress was calculated using the maximum stress developed within the inner span, according to the following equation:

$$\sigma = \frac{3PD}{h^2d}$$

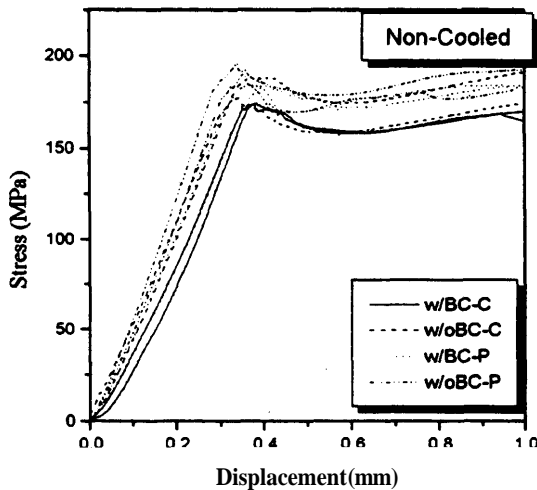
where P is the applied load, D is the distance between the loading and support bar (10 mm), h is the thickness, and d is the width of the bar. Displacement was determined using the values measured from the crosshead motion (excluding the set-up compliance). The calculated stress is the tensile force that is present on the ceramic surface (also referred to as the outer fiber stress). It should be noted that the calculation of the stress assumes the coating-substrate composite system as one material, allowing the applied bending loads to be normalized with respect to the variations in the sample thickness and width. Hence, a direct comparison of these cooled and non-cooled samples is only possible from the load-displacement curves; but in such a case different sample dimensions will need to be taken into account.

All the curves in Fig. 1 show an initial linear range, which then changed to a non-linear portion, indicative of an elastic-plastic response. The initial non-linear "toe" region can also be recognized, and is attributed to the arrangement of the loading and support bars on the sample. This behavior of the composite system arises since the composite consists originally of a steel substrate and in some instances a metallic bond coat. Hence, the transition from the elastic to plastic regions can be related to the behavior of the metal substrate, with the deformation characteristics of the metal substrate dominating after yielding.

The presence of the ceramic coating, together with the bond coat layer where applicable, has a significant influence on the stress-displacement curve prior to yield. This can be recognized by the presence of a peak transition region between the elastic and plastic portions when the coating is present on the substrate, suggesting that the coating is structurally contributing to the material responses of the composite structure until yielding. Therefore, this behavior indicates that the coating is inhibiting yield of the composite system with respect to the usual behavior of the metal substrate where there is a smooth transition region. Thus, the coating appears to reinforce or strengthen the system and the yield point is elevated. Accordingly, the peak stress can be related to the failure



(a)



(b)

Fig. 1 Stress-displacement curves from four-point bending tests (a) for cooled and (b) non-cooled samples. The figures include samples having bond coat ("w/BC") or no bond ("w/oBC") coat layer which are either sprayed continuously ("C") or with pauses ("P").

of the coating [15]. It should also be noted that the peak load behavior is more pronounced for the "non-cooled" coatings.

The changes in the yield stress for samples sprayed with and without a bond coat layer, for the cooled and noncooled cases having a continuous and paused spray structure is shown in Fig. 2. A three-level analysis of variances (ANOVA) test on the data indicated that the cooling and pausing features are statistically significant factors that have an effect on the yield stress results. The influence of these variables will also be shown and discussed for the AE results. A significant feature which is not highlighted by the statistical analysis results but can be recognized from Fig. 2 is that a larger variation in the average yield stresses is present for samples with no bond coat layer (can be observed as an increasing trend in the figure) while the bond-coated samples have more equivalent results. This indicates that (i) the presence of the bond coat has a critical influence on the results, and (ii) the application of cooling or no cooling and any pauses during spraying has a more significant effect on samples having no bond coat layer applied. This behavior can be explained on the basis of the role of the bond coat layer, where, among its other features, it is also known [22] to act as a compliant layer in decreasing the thermal expansion mismatch between the ceramic coating and the metal

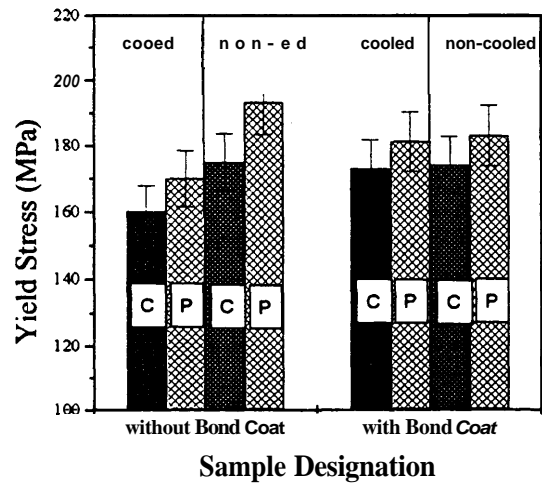


Fig. 2 Yield stress of the coating system determined from the four-point bending curves. The results are given for samples having a bond coat and no bond coat layer, which are sprayed either continuously ("C") or with pauses ("P").

substrate. The benefit from this behavior, which is normally intended to be dominant at high temperatures, is that the ceramic overlay is isolated from high strain and hence, is prevented from spallation [22]. For repeated thermal cycling, this continues until the bond coat can not plastically deform, i.e., creep. This reason for this behavior has been attributed to the increase in the strain energy release rate for buckling spallation and a corresponding decrease in critical flaw size for failure due to the formation of an oxide layer [23,24]. It is also argued that the depletion of aluminum from the bond coat results in an oxide layer other than α -alumina that have inferior mechanical properties and lead to failure [25].

Stresses arising in the ceramic layer during the initial cooling, on the other hand, are reported to be compressive in the ceramic [22] near to the ceramic-bond coat interface. This behavior depends on the other processing parameters; specifically on the substrate temperature [26,27]. The application of cooling or no cooling during spraying, thus, is related directly to the substrate temperature. Accordingly, cooling, whether it is applied or not, can be expected to influence the ceramic coating and the interfaces that it abuts (either the bond coat or substrate). It will be shown with the indentation analysis that the influence of cooling has a greater influence on the bond coat layer and the bond coat-ceramic interface.

Another significant feature that is recognized from Fig. 2 is that the samples sprayed with pauses all tend to exhibit a higher yield stress compared to the continuously sprayed coatings of the same thickness. It is quite likely that there are stresses concentrated at the interfaces that are formed during the spray interruption. This is illustrated in Fig. 3 where the crack which has originated from the surface has deflected at the interface where the coating cycle was paused that is close to the bond coat layer. A similar behavior of thermal spray coatings under indentation stresses was shown in another study [28,29]. Apparently, the presence of these regions contributes to the improvement in the low temperature integrity of the composite system.

The total AE events recorded during the linear elastic portion of bending for the various samples are shown in Fig. 4. The elastic region AE events are investigated to study the deformation characteristics of the ceramic coating since after yielding the ceramic coating is known to fail during bending. For the continuous sprayed coatings, cooling and the presence of a bond-coat layer causes lower AE activity during bending compared to the non-cooled coatings. Similar behavior was shown and discussed in another study for a different coating thickness [15], where residual

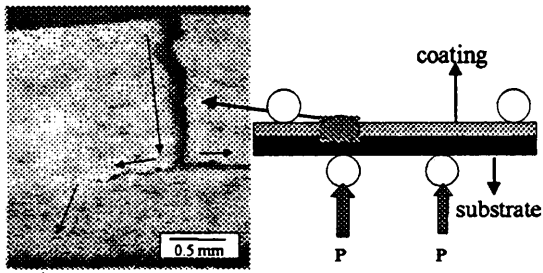
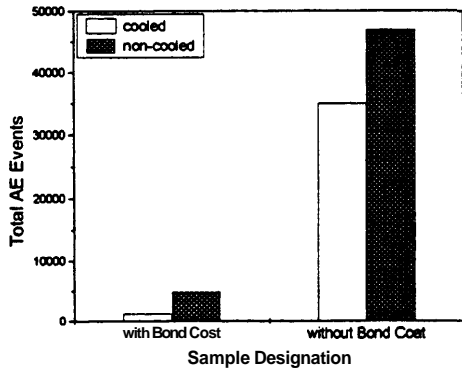
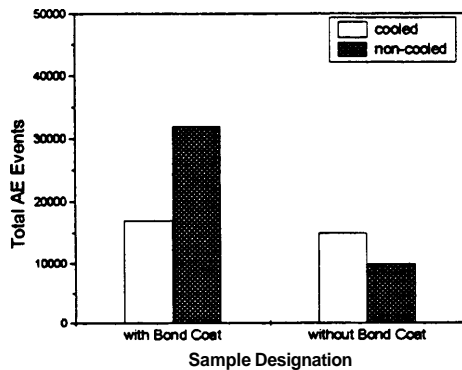


Fig. 3 Side view of sample deformed using four-point bending, showing cracks that have originated from the surface at the high stress region and have propagated until it was deflected at the interface formed by the pauses during spraying

stresses and absorption of AE activity [10] were factors responsible for this behavior. When the coating is sprayed with pauses, the most significant feature recognized is the decrease in the total AE activity for the non-bond coated samples and an increase for the bond-coated samples, both compared with the continuously sprayed coatings. Also, the cracking events for the non-continuously sprayed coatings with and without bond coat are reasonably equivalent when compared with the continuous coatings. Hence, it can be concluded that discontinuities during spraying tend to create a layered structural formation (see Fig. 3), which causes cracking during elastic deformation in a similar way for both the bond coated and non-bond coated samples. At this point, it is difficult to explain this behavior using only the mechanical and acoustic responses of the samples. However, the layered formation in the coating, which is seen to strongly influence the mechanical characteristics of the coating, most likely relates to



(a)



(b)

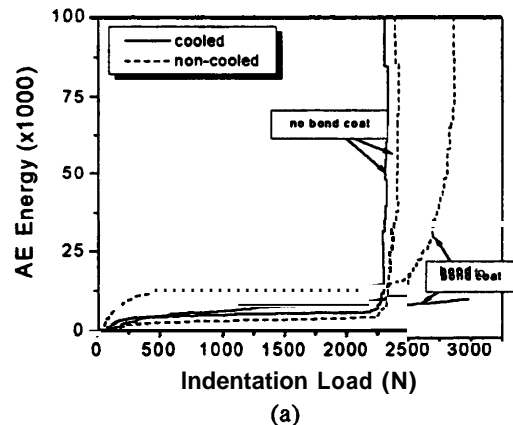
Fig. 4 Total number of AE events for four-point bending samples detected before yielding, for samples that are sprayed (a) continuously and (b) with pauses

the stress distribution in the ceramic coating that is largely affected by the temperature variations caused by the pauses.

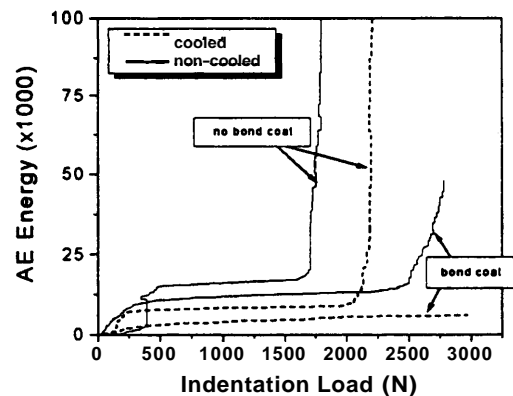
Hertzian Indentation and Acoustic Emission. The acoustic emission energy response for the cooled and non-cooled samples, with and without the presence of a bond coat layer, for coatings that are continuously or non-continuously sprayed is shown in Fig. 5. It should be noted that, although a total of six indentations were performed and analyzed for each condition, only one representative result was selected and is shown in the figure to illustrate the trends detected. One significant feature that is recognized from the curves is that there is a critical load (L_c) after which the AE energy increases dramatically. This load has been correlated with the failure of the coating under the large stresses. Table 2 shows these loads for all the spraying conditions applied in this study.

The failure, where applicable, has been detected to be in the form of radial cracks emanating from the indentation area or as spallation/removal of the coating from the substrate. Note that not all the samples show this behavior. Coatings with a bond coat layer that were cooled during spraying did not fail until the maximum load (3 kN) applied in this study. This correlates well with the bending results discussed in the previous section as well as with previous studies [15]. It was noted in these discussions that the presence of the bond coat layer suppresses AE activity [10] due to surface compressive stresses inhibiting cracks. The indentation results, in support of the bend test results and application experience, verify that the bond coat layer improves the overall integrity of the TBC system.

On examining Fig. 5, it is observed that the critical load is higher when a bond coat layer is present for both the continuously and non-continuously sprayed coatings. This, being in good agreement with the bending results supports the well-accepted concept



(a)



(b)

Fig. 5 AE energy versus indentation load for samples that are sprayed (a) continuously and (b) with pauses

Table 2 Critical load, " L_{cr} ", defining the onset of larger AE activity

	Continuous sprayed	Paused sprayed
Cooled		
With bond coat	>3000	>3000
Without bond coat	2000	2200
Non-Cooled		
With bond coat	2500	2500
Without bond coat	1650	2250

that the bond coat is a major constituent in contributing to the integrity of the TBC system. It is known that during Hertzian indentation, the stresses below the indenter are compressive during loading while the surrounding area is in tension [30]. Hence, the coating below the indenter is compressed while its surroundings are pulled apart. Accordingly, when the loads are large enough, the coating fails mainly due to the tensile stresses that cause the pre-existing cracks to grow and the pores to coalesce. Thus, when the bond coat layer is present, such cracks are prevented from forming and growing, and confer good coating integrity.

The effect of discontinuities during spraying has been more significant for samples that have no bond coat, where decreases in the critical load, L_{cr} , can be noted; and has been especially significant for the non-cooled sample. Another characteristic for these samples is that both exhibit an initial step in the energy versus load curve at loads lower than 500N. The fact that the discontinuities during spraying cause a layered coating has been suggested in the previous discussions. This idea is once more strengthened with the indentation AE data, where more cracking is noted for these layered coatings. The initial step in the AE response can be correlated with the layered structure, most probably to cracks forming and growing between the layers. Also, cooling during spraying was shown to form a stronger coating in a former study [10], most probably due to surface compressive stresses. This is again supported with the larger L_{cr} for the cooled sample with the layered coating, compared with the non-cooled sample, both having no bond coat layer.

Conclusions

The yield stress from the bending tests and the indentation loads leading to coating failure together with the deformation characteristics of coating-substrate system are shown to be significantly influenced by external cooling, the spraying procedure (continuous or paused), and by the presence of a bond coat layer. It is shown that the bending deformation behavior of coatings can be used as a simple guide to gain information about the integrity of the coating-substrate composite systems and, more importantly, the characteristics of the coating deformation behavior. Using this analysis, changes in the mechanical response of the composite are observed with respect to influences of various spray parameters and processing methods. The combination of these parameters are factors that determine the mechanical properties and, hence, the failure characteristics of the coatings.

On the other hand, it is shown that the influence of processing parameters are more striking on the AE behavior. The AE analysis during bending and Hertzian indentation tests shows that the cracking phenomena in these samples change, depending on the processing parameters used. For bending studies, the deformation during the elastic region is significant in determining the fracture characteristics. For indentation, the critical load where the structure fails is determined and is shown to be related significantly to the spraying parameters without extracting information from the load-displacement behavior [28,29]. The overall analysis of the results indicate that coating adhesion and integrity and residual stresses play a major role on the influence of mechanical and

deformation characteristics of the system as a function of any cooling application and presence of bond coat layer. The influence of the bond coat layer in improving the mechanical adhesion and coating integrity, the application of cooling to strengthen the coating, and obtaining a less flawed coating with a continuous spraying procedure are shown as significant characteristics of the coating that can be ascertained from bending and indentation tests.

Acknowledgments

C. R. C. Lima would like to thank FAPESP-Brazil for the financial support during his stay at SUNY Stony Brook. R. S. Lima acknowledges the support of an ITSA scholarship. This work was sponsored under NSF-MRSEC DMR, grant number 9632570.

References

- [1] Pawlowski, L., 1995, *The Science and Engineering of Thermal Spray Coatings*, Wiley, New York.
- [2] Taylor, R., Brandon, J. R., and Morrel, P., 1992, "Microstructure, Composition and Property Relationships of Plasma-Sprayed Thermal Barrier Coatings," *Surf. Coat. Technol.*, **50**, pp. 141-149.
- [3] Clyne, T. W., and Gill, S. C., 1996, "Residual Stresses in Thermal Spray Coatings and Their Effect on Interfacial Adhesion: a Review of Recent Work," *J. Thermal Spray Technol.*, **5**, pp. 401-418.
- [4] Clyne, T. W., and Gill, S. C., 1994, "Investigation of Residual Stress Generation During Thermal Spraying by Continuous Curvature Measurement," *Thin Solid Films*, **250**, pp. 172-180.
- [5] Kuroda, S., Dendo, T., and Kitahara, S., 1995, "Quenching Stress in Plasma Sprayed Coatings and its Correlation with the Deposit Microstructure," *J. Thermal Spray Technol.*, **4**, pp. 75-84.
- [6] Zhou, Z., Eguchi, N., and Ohmori, A., 1997, "Microstructure Control of Zirconia Thermal Barrier Coatings by Using YAG Laser Combined Plasma Spraying Technique," *Thermal Spray: A United Forum for Scientific and Technological Advances*, C. C. Berndt, ed., ASM International, Materials Park, OH, pp. 315-321.
- [7] Lima, C. R. C., and Trevisan, R. E., 1997, "Graded Plasma Spraying of Premixed Metal Ceramic Powders on Metallic Substrates," *J. Thermal Spray Technol.*, **6**, pp. 187-192.
- [8] Tsui, Y. C., and Clyne, T. W., 1996, "Adhesion of Thermal Barrier Coating Systems and Incorporation of an Oxidation Barrier Layer," *Thermal Spray: Practical Solutions for Engineering Problems*, C. C. Berndt, ed., ASM International, Materials Park, OH, pp. 275-284.
- [9] Bordeaux, F., Moreau, C., and Saint Jacques, R. G., 1992, "Acoustic Emission Study of Failure Mechanisms in TiC Thermal Barrier Coatings," *Surf. Coat. Technol.*, **54/55**, pp. 70-76.
- [10] Shankar, N. R., Berndt, C. C., Herman, H., and Rangaswamy, S., 1983, "Acoustic Emission from Thermally-Cycled Plasma-Sprayed Oxides," *Am. Ceram. Soc. Bull.*, **62**, pp. 614-619.
- [11] Zhang, H. T., Zhou, X. K., Guan, K., Liao, B., and Cao, S., 1987, "Acoustic Emission Research on the Fracture Behavior of Plasma-Sprayed Ni-Al Coatings During Bend Testing," *Surf. Coat. Technol.*, **30**, pp. 115-123.
- [12] Berndt, C. C., Robins, D., Zatorski, R., Herman, H., 1983, "Fire Barrier Coatings for Protection of Aluminum Structures," *Proceedings of the 10th International Thermal Spraying Conference*, DVS Berichte, Dusseldorf, pp. 182-186.
- [13] Lin, C. K., Berndt, C. C., Leigh, S., and Murakami, K., 1997, "Acoustic Emission Studies of Alumina-13 percent Titania Free-Standing Forms During Four-Point Bend Tests," *J. Am. Ceram. Soc.*, **80**, pp. 2382-2394.
- [14] Lin, C. K., 1995, "Statistical Approaches to Study Variations in Thermal Spray Coatings," *Ph.D. thesis*, State University of New York at Stony Brook, Stony Brook, NY.
- [15] Senturk, U., Lin, C. K., Lima, R. S., Lima, C. R. C., and Berndt, C. C., 1999, "Processing and Mechanical Properties of Plasma Sprayed Thermal Barrier Coatings," to be published in the 1999 United Thermal Spray Conference Proceedings.
- [16] Berndt, C. C., Phucharoen, W., and Chang, G. C., 1984, "The Mechanical Properties of Thermal Barrier Coatings Used for Gas Turbine Blades," *Turbine Engine Hot Section Technology*, NASA Workshop, pp. 155-166.
- [17] Berndt, C. C., 1988, "Cracking Processes in Thermally Sprayed Ceramic Coatings," *Mater. Sci. Forum*, **34-36**, pp. 457-461.
- [18] Shankar, N. R., Berndt, C. C., and Herman, H., 1983, "Structural Integrity of Thermal Barrier Coatings by Acoustic Emission Studies," *Proceedings of the 10th International Thermal Spraying Conference*, DVS Berichte, Dusseldorf, pp. 41-45.
- [19] Shankar, N. R., Berndt, C. C., and Herman, H., 1983, "Characterization of the Mechanical Properties of Plasma-Sprayed Coatings," *Materials Science Research Advances in Materials Characterization*, Plenum Press, New York, NY, **15**, pp. 473-489.
- [20] Shankar, N. R., Berndt, C. C., and Herman, H., 1982, "Failure and Acoustic Emission response of Plasma-Sprayed ZrO₂-8wt percent Y2O₃ Coatings," *Ceram. Eng. Sci. Proc.*, **3**, pp. 772-792.

- [21] Safai, S., Herman, H., and Ono, K., 1980, "Acoustic Emission Study of Thermally Cycled Plasma Sprayed Oxide Coatings," *Proceedings of the 9th International Thermal Spraying Conference*, Netherlands Instituut voor Lastechniek, pp. 1291-132.
- [22] Bennet, A., 1986, "Properties of Thermal Barrier Coatings," *Mater. Sci. Technol.*, **2**, pp. 257-261.
- [23] He, M. Y., Evans, A. G., and Hutchinson, J. W., 1996, "Interface Cracking Phenomena in Constrained Metal Layers," *Acta Mater.*, **44**, No. 7, pp. 2963-2971.
- [24] He, M. Y., Evans, A. G., and Hutchinson, J. W., 1998, "Effects of Morphology on the Decohesion of Compressed Thin Films," *Mater. Sci. Eng., A*, **A245**, No. 2, pp. 168-181.
- [25] Brindley, W. L., and Whittenberger, J. D., 1993, "Stress Relaxation of Low Pressure Plasma-Sprayed NiCrAlY Alloys," *Mater. Sci. Eng., A*, **A163**, No. 1, pp. 33-41.
- [26] Bianchi, L., Luchesse, P., Denoirjean, A., and Fauchais, P., 1995, "Zirconia Splat Formation and Resulting Coating Properties," *Proceedings of the 8th National Thermal Spray Conference*, C. C. Berndt and S. Sampath, eds., ASM International, Material Park, OH, pp. 261-266.
- [27] Bianchi, L., Luchesse, P., Denoirjean, A., Fauchais, P., and Kuroda, S., 1995, "Evolution of Quenching Stress During Ceramic Thermal Spraying with Respect to Plasma Parameters," *Proceedings of the 8th National Thermal Spray Conference*, C. C. Berndt and S. Sampath, eds., ASM International, Material Park, OH, pp. 267-271.
- [28] Pajares, A., Wei, L., Lawn, B. R., and Berndt, C. C., 1996, "Contact Damage in Plasma-Sprayed Alumina-Based Coatings," *J. Am. Ceram. Soc.*, **79**, pp. 1907-1914.
- [29] Pajares, A., Wei, L., Lawn, B. R., Padture, N. P., and Berndt, C. C., 1996, "Mechanical Characterization of Plasma Sprayed Ceramic Coatings on Metal Substrates by Contact Testing," *Mater. Sci. Eng., A*, **A208**, pp. 158-165.
- [30] Fischer-Cripps, A. C., and Lawn, B. R., 1996, "Stress Analysis of Contact Deformation in Quasi-Plastic Ceramics," *J. Am. Ceram. Soc.*, **79**, pp. 2609-2618.

Journal of Engineering for Gas Turbines and Power

Published Quarterly by The American Society of Mechanical Engineers

VOLUME 122 • NUMBER 3 • JULY 2000

365 In Memoriam: Professor James E. Peters

Gas Turbines: Aircraft

366 Computational Simulation of Gas Turbines: Part 1—Foundations of Component-Based Models (99-GT-346)

John A. Reed and Abdollah A. Afjeh

377 Computational Simulation of Gas Turbines: Part 2—Extensible Domain Framework (99-GT-347)

John A. Reed and Abdollah A. Afjeh

Gas Turbines: Ceramics

387 Deformation of Plasma Sprayed Thermal Barrier Coatings (99-GT-348)

Ufuk Senturk, Rogerio S. Lima, Carlos R. C. Lima, and Christopher C. Berndt

393 Effects of Alloy Composition on the Performance of Ytria Stabilized Zirconia—Thermal Barrier Coatings (99-GT-350)

Josh Kimmel, Zaher Mutasim, and William Brentnall

401 Reductions in Acquisition Costs for State-of-the-Art Fabrication of CFCC Turbine Engine Combustor Liners (99-GT-352)

Phillip A. Craig and David Godfrey

Gas Turbines: Combustion and Fuel

405 An Experimental and Modeling Study of Humid Air Premixed Flames (99-GT-8)

Anuj Bhargava, Med Colket, William Sowa, Kent Casleton, and Dan Maloney

412 Passive Control of Combustion Instability in Lean Premixed Combustors (99-GT-52)

Robert C. Steele, Luke H. Cowell, Steven M. Cannon, and Clifford E. Smith

420 Combustion Instabilities in Industrial Gas Turbines—Measurements on Operating Plant and Thermoacoustic Modeling (99-GT-110)

David E. Hobson, John E. Fackrell, and Gary Hewitt

Gas Turbines: Cycle Innovations

429 Natural Gas Fired Combined Cycles With Low CO₂ Emissions (99-GT-370)

Paolo Chiesa and Stefano Consonni

437 Handling of a Semiclosed Cycle Gas Turbine With a Carbon Dioxide-Argon Working Fluid (99-GT-374)

Inaki Ulizar and Pericles Pilidis

Gas Turbines: Heat Transfer

442 Performance of Pre-Swirl Rotating-Disc Systems

Hasan Karabay, Robert Pilbrow, Michael Wilson, and J. Michael Owen

Gas Turbines: Manufacturing, Materials, and Metallurgy

451 Stress Relaxation Testing of Service Exposed IN738 for Creep Strength Evaluation (99-GT-285)

David A. Woodford

(Contents continued on inside back cover)